# General Disclaimer

One or more of the Following Statements may affect this Document

- This document has been reproduced from the best copy furnished by the organizational source. It is being released in the interest of making available as much information as possible.

- This document may contain data, which exceeds the sheet parameters. It was furnished in this condition by the organizational source and is the best copy available.

- This document may contain tone-on-tone or color graphs, charts and/or pictures, which have been reproduced in black and white.

- This document is paginated as submitted by the original source.

- Portions of this document are not fully legible due to the historical nature of some of the material. However, it is the best reproduction available from the original submission.
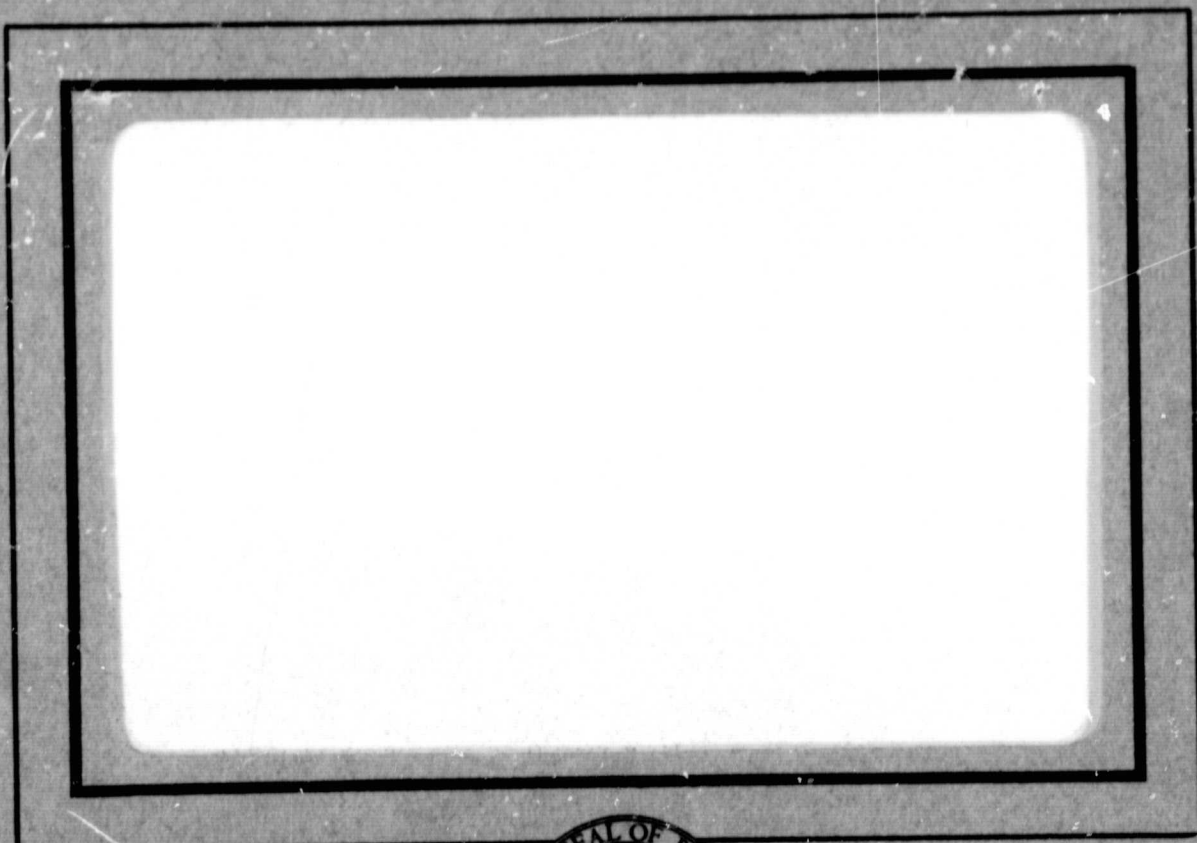
DEPARTMENT OF

SPACE SCIENCE

🦉 🦉 🦉

RICE UNIVERSITY

HOUSTON, TEXAS

FINAL SCIENTIFIC REPORT

NASA GRANT NGR-44-006-044

FEASIBILITY STUDY

OF

LUNAR NEUTRON ALBEDO EXPERIMENT

Submitted to:

National Aeronautics and Space Administration
Washington, D. C.   20546

Submitted by:

Department of Space Science
Rice University
Houston, Texas   77001

January, 1969

Robert C. Haymes
Principal Investigator

SUMMARY

Cosmic rays interacting with the surface nuclei of the moon
produce neutrons, some of which emerge from the surface. The energy
spectrum of this emergent albedo will depend strongly on the
composition of the surface, especially upon concentrations of
hydrogen. A measurement of the ratio of the slow to fast neutron
counting rates will serve as an index of the hydrogen content in
the lunar surface.

A feasibility study is made on the effect on the slow and
fast neutron counting rates due to increases in water content.
A lunar neutron simulator, consisting of neutron detectors and
a fast neutron source, measures the effect of water concentration
on the ratio using a baslatic material like that found on the moon
by the Surveyors. A sand-water mixture was also used in order to
demonstrate the effects of differing elemental compositions in the
sample.

Data obtained using a 0.3% water content (by weight) in basalt
indicate an increase of about 4% in the ratio over the 0.2% water conte
level. As expected from theory, the variation in ratio with water
concentration is quite linear, for both samples tested. The
only effect of variations in the elemental composition is to alter
the slope of the line.

We conclude that the experiment as proposed is sufficiently sensitive to detect a variation in water concentration of 0.1% (by weight). Since the least concentration of water expected is ~0.1% (the amount found in stony meteorites) and the concentration may be ~ the 1% found in volcanic rock, it appears that the lunar neutron albedo experiment will serve as a valuable tool in remotely prospecting the lunar surface for hydrogen matter such as water.

I. INTRODUCTION

A. Lunar Neutrons

Neutron production within the surface of the moon can be used as an indicator of the presence of hydrogen in the material of the lunar crust. The neutrons are produced by the interaction of cosmic rays and the surface material. The neutrons are scattered isotropically and some may escape the surface of the moon. This emergent flux is known as the lunar neutron albedo.

The production of neutrons with a large fast component (several Mev) in a medium of low neutron capture cross section creates a process of "thermalization". The fast neutrons lose energy due to collisions with the sub-surface nuclei until the neutrons have velocities characteristic of "slow" neutrons. Therefore, the lunar albedo consists of varying neutron energies dependent on the scattering nuclei of the material.

Elastic scattering has a strong dependence on the atomic weight of the scattering center, the loss being greatest for hydrogen. Consider the simple collision of a neutron with a nucleus in the center-of-mass coordinates as follows:

$$E_2 = (M-m)^2/(M+m)^2 \times E_1$$

E_2 is the energy of the neutron after the collision with a nucleus of mass M; E_1 is the energy before the collision and m is the mass of the neutron (Rusk, 1964). For a head on collision of a neutron with a proton at rest, the above

equation shows that the neutron loses all of its energy and momentum with the momentum and kinetic energy being transferred to the proton. However, since random collisions occur at varying angles, the neutron will lose on the average only 63 percent of its energy per collision. After two such collisions, the neutron would have only 14 percent of its original energy. A 2-Mev neutron can be reduced to thermal energies in about 18 collisions in hydrogen (Rusk, 1964). The average number of collisions needed to reduce the energy of a neutron from one value E_2 to any value E is given by

$$N = \ln(E_2/E)/\xi$$

where ξ is defined as the average decrease in the logarithm of energy per collision, i.e., $\xi \circeq \ln(E_2/E)$. ξ for hydrogen has a value of 1; for carbon, $\xi \circeq 0.16$ (Soodak, 1962). In the case of isotropic scattering in the CM system, the ξ for A > 10 is approximately $2/(A + .67)$. Hence, the neutrons that emerge from the surface of the moon depend strongly on the atomic weight of the scattering centers. Hydrogen will produce a high flux of slow neutrons if it appears in the sub-surface material.

B.   Review of Neutron Scattering Theory

Elastic scattering is usually the only process which occurs with neutrons of a few Mev or less and elements of low A, i.e., $A \leq 25$. At higher energies the scattered neutron has less energy than the incident neutron; the difference is used in nuclear excitation. Usually a gamma ray is released in the de-excitation process. However, in the low A elements, the lowest excited state is very high (many Mev), hence, only elastic scattering occurs (Price, 1958).

As the fast neutrons traverse matter and lose energy, the process of thermalization is established. If the medium has a low absorption cross section, a Maxwellian distribution will arise from the motion of the scattering atoms and the thermal neutrons. This, however, is not exactly true since some absorption will prevail and there will be leakage before thermalization. For a low A material which weakly absorbs, the neutron energy distribution approximates an equilibrium distribution. This Maxwellian distribution can be represented as follows:

$$N(E)dE = 2\pi n/(\pi kT)^{3/2} e^{-E/kT}$$

The average energy is $(3/2)kT$ while the most probable velocity is $(2kT/m)^{\frac{1}{2}}$. At $T = 293.6K°$, $E = kT = .253$ ev; the most probable velocity is 2200 m/sec. The total flux is given by $\phi = \int_0^a N(v)dv_v = n\bar{v} = \int \rho dv$ where ρ is the density of neutrons.

When the slow neutrons approach the nucleus they come within range of nuclear forces. If such a neutron is "attracted" by these forces it can be captured. Usually the excited nucleus emits a gamma ray; this is called radiative capture (Isbin, 1963). The presence of a neutron with an energy near the resonance energy increases the probability of capture. However, most of the resonance capture is for higher A elements. A medium with a low absorption cross section and a low atomic weight will mainly produce leakage. This leakage will be affected by capture mainly at slow neutron energies when the capture cross sections become important.

If a fast neutron source is placed near an absorbing-scattering material with the neutron beam essentially parallel, the transmitted neutron intensity I is related to the incident intensity I_o by the exponential equation (Title, 1964).

$$I = I_o e^{-N\sigma x}$$

where N is the number of atoms/cm^3 in the absorber, σ is the total microscopic neutron cross section (cm^2/atom) and x is the sample thickness. The energies of the incident and transmitted neutrons are the same. For more than one type of atom, a summation over N and σ is necessary. This summation is denoted by Σ_t, the total macroscopic neutron cross section.

The preceding provides many essentials for the problem of slowing down of neutrons. As the neutrons diffuse and scatter through the medium, the energies correspondingly

change. The number per unit volume whose energy has changed to E per unit time is the slowing down density q. The relation between q and the flux is as follows: (Title, 1964)

$$q = \phi \, \xi \Sigma_s$$

where Σ_s is known as the "slowing down power" of the medium. ξ is the mean logarithmic energy loss per collision.

In a medium which produces thermalization, multi-group diffusion theory may be applied. In its simplest form, multi-group reduces to one-group where group refers to neutrons at the same energies. This is a low-order approximation of transport theory in that the neutrons of constant energy diffuse through a medium. The differential equation of diffusion theory is as follows (Glasstone and Edlund, 1952):

$$D \, \nabla^2 \phi - \frac{\phi}{\lambda_a D} + S = \frac{\partial n}{\partial t}$$

Here ϕ is the neutron flux in neutrons/cm^2-sec, λ_a the absorption mean free path, D the diffusion coefficient, S the source strength per unit volume, n the neutron density in neutrons per unit volume, and t is the time. The neutron flux is related to the neutron speed v, as follows:

$$\phi = nv$$

The neutron density in the steady state is constant in time, hence the right hand side of the above equation is equal to zero. Usually there is a point source; at all points except the origin S is zero. The above equation may then be written

$$\nabla^2 \phi - \frac{\phi}{\lambda_a D} = 0$$

The diffusion length L is defined as $(\lambda_a D)^{\frac{1}{2}}$. Thus

$$\nabla^2 \phi - \frac{\phi}{L^2} = 0$$

D is defined as $\frac{\lambda_{tr}}{3}$ where λ_{tr} is the transport mean free path given by $\frac{\lambda}{(1-\overline{\cos\theta})}$. λ is the total mean free path and $\overline{\cos\theta}$ is the average cosine of the scattering angle in the laboratory system. In the CM system, $\overline{\cos\theta} = 2/3(A)$, hence

$$\lambda_{tr} = \frac{\lambda}{(1-2/3[A])}$$

For a description of slowing down using one group diffusion theory, the "slowing down power" is used in place of the absorption mean free path. L then represents the slowing down length for epithermals, i.e., neutrons with energies from 0.1-100 ev. The solution of the one group equation for a point source in an infinite homogenous medium is (Feld, 1953)

$$\phi = \frac{\phi}{4\pi D} \frac{e^{-r/L}}{r}$$

where ϕ is the epithermal of slowing down flux, or it is the thermal flux, depending on the energy.

C.   Expected Lunar Intensities

The neutrons that are produced on the surface of the
moon are a result of interactions of cosmic rays with the
surface nuclei. Fig. 1 shows the observed solar (Fichtel,
1963) and galactic cosmic rays proton flux. Without a
magnetic field or an atmosphere, the charged particles
(mainly protons) of low energy are not deflected away
from the moon, hence, there are direct interactions be-
tween the primaries and the surface nuclei. The flux may
be like that found near the geomagnetic poles of the Earth.
The nuclear reactions are complex which include meson
production, evaporation, and knock-on mechanisms.

It should be noted that the production of neutrons at
the surface of the moon is about five times that of the
global average of the Earth (Lingenfelter, Canfield and
Hess). Besides the high incident cosmic ray flux, the
average atomic weight of the surface of the moon is
higher than the Earth's atmosphere. Also, pions created
in the primary interactions may interact before decaying.
All of the preceding generate the increased production
value. An approximation of the lunar albedo can be made
by scaling the value of the terrestrial albedo (Haymes
and Korff, 1960). The slow neutron density near 40 degrees
geomagnetic latitude is 1×10^{-8} neutrons/cm^3. Later
measurements of the fast albedo revealed the flux to be
approximately 0.1/cm^2/sec at geomagnetic latitude of 41
degrees.

The neutrons produced on the lunar surface result
from inelastic processes in excited nuclei. Gamma rays,

(Fichtel, Guss & Ogilvie 1963)

VARIOUS SOLAR
PARTICLE SPECTRA

GALACTIC COSMIC RAYS
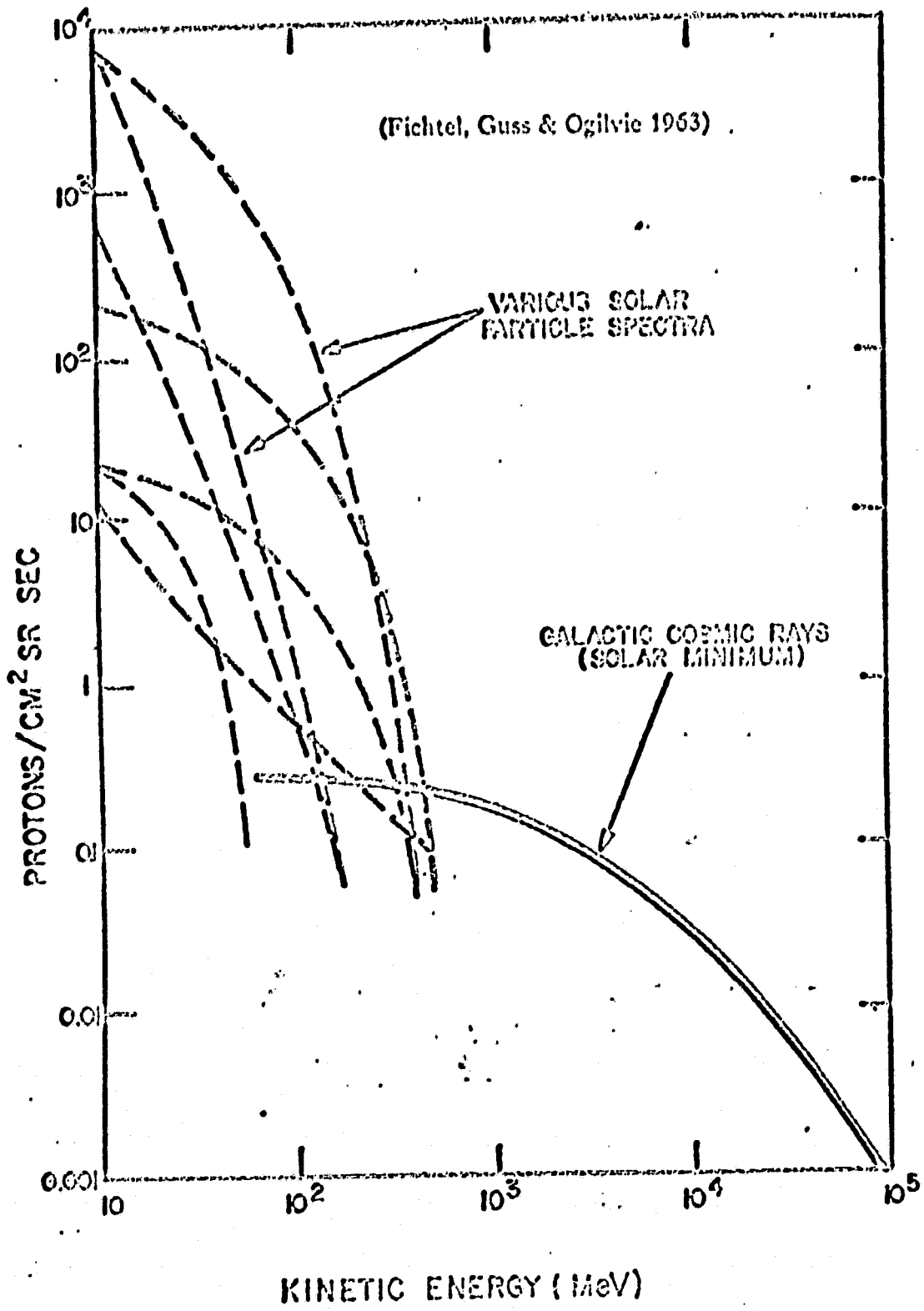(SOLAR MINIMUM)

KINETIC ENERGY (MeV)

Fig 1

charged particles, and neutrons are a direct result of
the interactions. The neutrons can be captured and
produce gamma rays or escape the surface of the moon.
Lingenfelter, Canfield and Hess (1962) used diffusion
theory to estimate the lunar neutron albedo. The cal-
culated equilibrium leakage spectrum produced is dependent
on the assumed composition and very sensitive to the
hydrogen concentration. The most significant result is
that of the ratio of slow to fast neutrons varies with
the variation of the ratio of hydrogen to silicon atoms.
(Silicon is used as a basis because [Si] is the parameter
in geological theories.)

In an experiment that would measure such a ratio
of slow to fast neutrons from the lunar surface, the
thermal neutron cross section would need to be known in
order to interpret the results in terms of the absolute
hydrogen concentration.

The lunar neutron flux will depend on the cross
sections and on the hydrogen content. The hydrogen
can be in the form of water of crystallization and/or
in the form of ice.

Approximately 0.5% of the lunar surface is believed
to be permanently shaded (Watson et al., 1961), and
fossil ice would remain at such sites. Volcanic rocks
have a water concentration of about 1% by weight while
stony meteorites have about 0.1% by weight (Green, 1964).
By correlating water concentration within the surface
of the moon, and the composition of the surface, a geological
connection can be made.

The experiment to be discussed herein employs a
simulator of lunar neutrons. By using a material similar

to that of the surface of the moon and be having a source
of fast neutrons, counting rate measurements are made of
the slow and fast neutrons as a function of the water
content in the material. A correlation is then made
between the ratio of the slow to fast neutron counting
rates and the water concentration.

Any significant statistical deviation in observed
counting rates can be then used as an index of hydrogen
concentration. Therefore, the purpose of this research
and thesis was to test the ideas outlined above and
establish quantitatively the sensitivity of the technique
to water concentration.

II. LUNAR NEUTRON SIMULATION

A. Simulator

The lunar neutron simulator consists of (fig. 2) a cylindrical drum with dimensions of 5 feet in length and 3 feet in diameter. The drum is mounted so that it can be rotated around the horizontal axis and also placed in a vertical position. It is sufficiently large so that over a ton of material may be loaded into it.

The three neutron detectors are located in the center of the drum at a distance of approximately 9 and 1/2 inches from the neutron source. The detectors are 120 degrees apart.

The neutron source used was a plutonium-beryllium radioactive source with a neutron yield of approximately 10^6 neutrons/sec. The distribution of energies is from 1 Mev - 10 Mev with the peak energy yield centered at 5 Mev. This source was similar to the neutrons produced on the lunar surface since the lunar neutrons are initially fast neutrons of several Mev.

The media used were a basaltic material from West Texas (a volcanic rock) and a finely washed variety of sand. These two samples were used so that the effects of differing elemental composition could be evaluated.

The drum was filled to a level of 4 feet from the lower end to insure proper neutron thermalization. This also gave a geometry which had equal amounts of material from source to detectors and source to surface.

NEUTRON SOURCE (Pu—Be)

ACCESS DOOR

BF₃ (B¹⁰) COUNTER
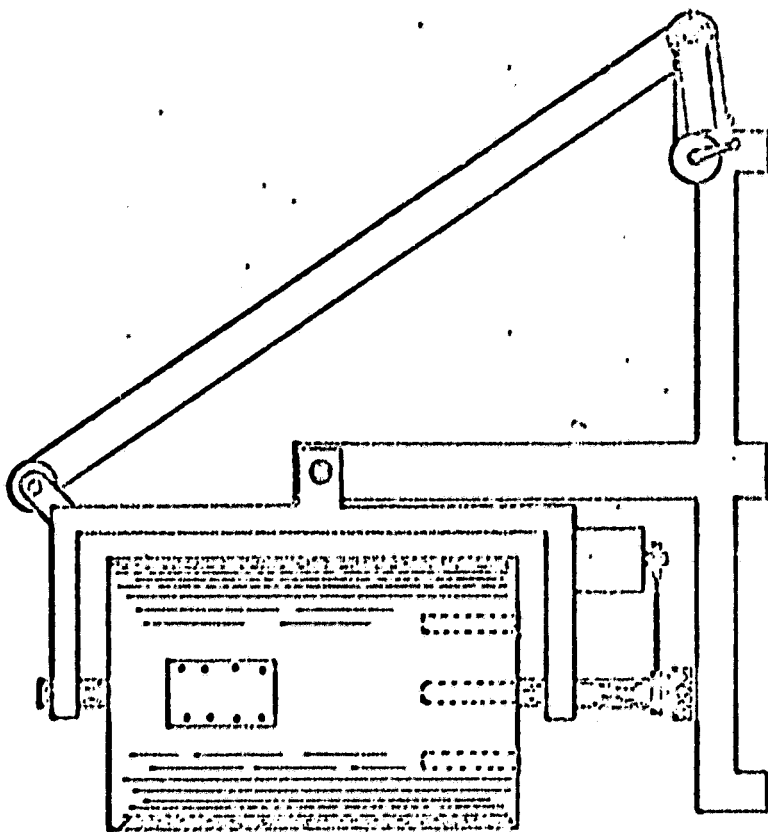
A

2F₃ (B") COUNTER

A

FAST NEUTRON SCINTILLATOR

Fig 2

Any level less than 4 feet would allow epithermal neutrons to leak from the top surface thereby losing these neutrons for counting.

The procedure used during the experiment was to use the drum in a horizontal position for mixing the material and the water. The drum has curved vanes which allow proper mixing and uniformity of water content. After mixing, the drum is placed in the vertical position so that the material may cover the detectors and the neutron source. Counting rates were obtained in this mode of the simulator.

B.   Neutron Detectors

Two unmoderated proportional counters filled with BF$_3$ were used as the slow neutron detector. The only difference between the counters is in the isotopic enrichment of the boron in the BF$_3$ gas. One counter has a concentration of 96% B^{10} while the other counter has a concentration of 11% B^{10} and 89% B^{11}. Boron-10 triflouride detectors utilize the B^{10} (n-α) reaction to detect slow neutrons. B^{10} has a high cross section for absorption of slow neutrons (1/v dependence; σ_α = 4000 barns). An alpha particle and lithium nucleus are products of this reaction; these charged particles produce the ionization in the counter. The ionizing power of the two particles is nearly the same so that the net pulse height is nearly equal to the pulse height due to alpha particles of energy 2.79 or 2.31 Mev. A 480 Kev gamma ray is liberated 94% of the time due to the decay of the lithium nucleus. The B^{11} isotope does not have an appreciable absorption cross section for slow neutrons; the preceding reaction does not take place (Blizard, 1962).

Both counters have a sensitive volume of 8 inches and a diameter of 2 inches. The fill pressure was 90 cm Hg with the measured plateau less than 2% per 100 volts (fig. 3). The operating voltage was found to be 3200 volts for both of the counters.

The difference of the counting rates in the two detectors is a measure of the slow neutron density.
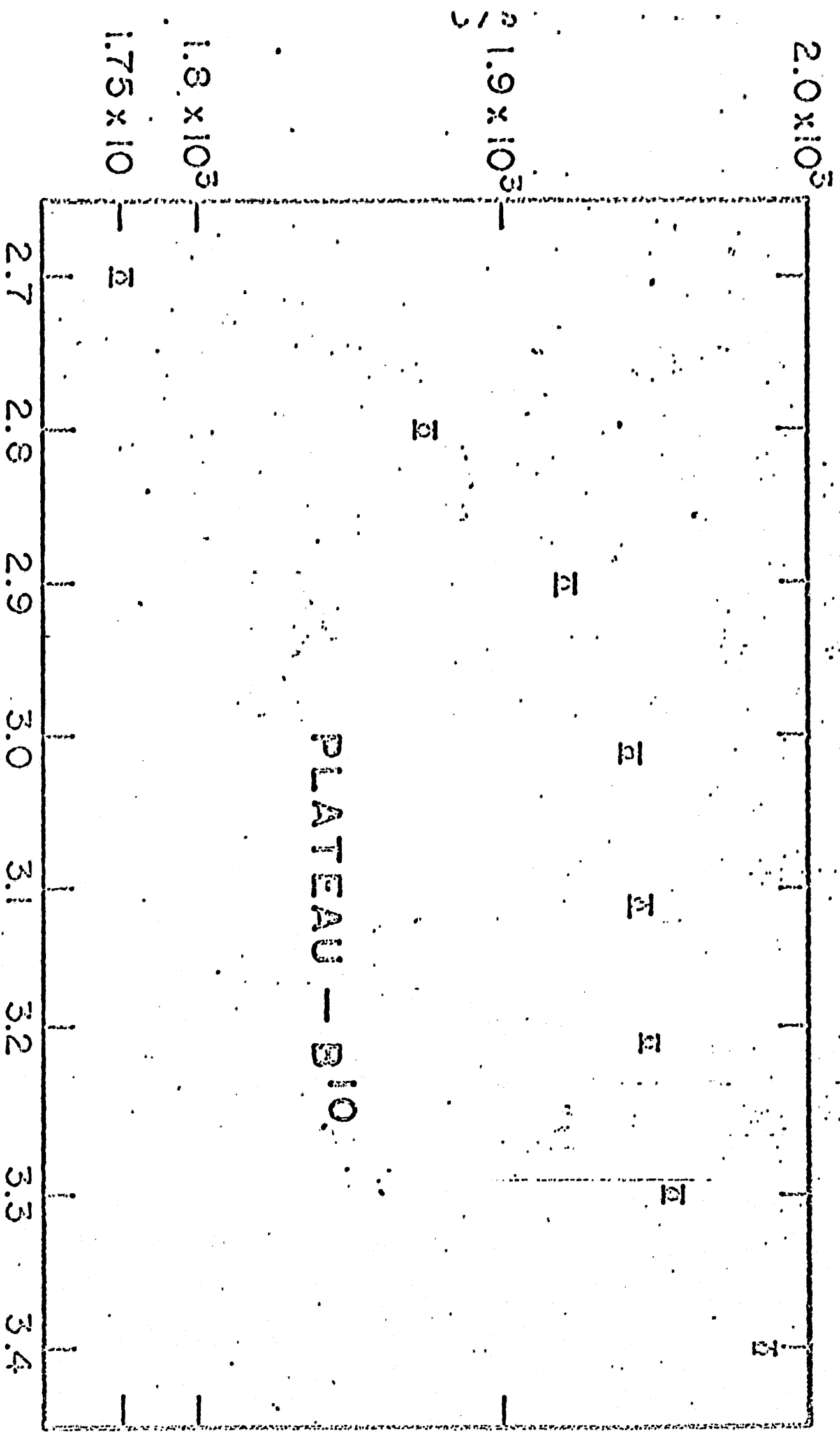
Fig 3

If n is the counting rate due to slow neutrons in a counter filled with 100% B^{10}, and b is the background counting rate due to charged particles, then

$$A = 0.96n + b$$
$$B = 0.11n + b$$

where A and B are the two measured counting rates of the two counters (Korff, 1945). These two equations may be solved for n and for the background counting rate b.

The fast neutron detector consists of an organic scintillator in which the neutron is detected through the (n,p) elastic scattering process. The scintillator has the property in that a neutron will lose some of its energy to the proton hence causing a pulse of light. A photomultiplier tube detects the light and the electronics acts upon this pulse (Haymes, 1965).

At the energies of fast neutrons, the scintillator also reacts to charged particles and gamma rays. Hence, a guard counter which consists of an inorganic scintillator surrounds the organic scintillator; this is called a phoswich system. Charged particles which traverse the two scintillators cause pulses to be generated in both layers. The pulses are differentiated from each other by pulse-shape dicsrimination. The gamma rays are also rejected through the pulse-shape discrinimation. The lower level of the detector is set at 1 Mev with the range being up to 15 Mev. The resolving time is 10 μ sec.

C.   Electronics

The two slow neutron detectors require a source
of high voltage, an amplification syste, and a counting
system.   The power supply used was a Fluke Corporation
model 408A which is an extremely well regulated, low
noise instrument.   The regulation is 0.001% for 10%
line change, with a ripple less than 1 mv RMS.

The amplification system consisted of an Ortec
103 preamp and 203 amplifier designed for use with solid
state radiation detectors.   This system has low noise
and the high sensitivity needed for the detectors.

The fast neutron detector required two small
power supplies for ± 8 volts and the counter.

The pulse from the (n, α) reaction is usually about
a millivolt at the output of the proportional counter.
Gamma rays generate fewer ions than do the neutrons.
The pulses due to the gamma background are much smaller
than the neutron pulses and are easily blocked by the
proper selection of the bias in the amplifier system.

The B^{10} counter has a maximum counting rate of
approximately 5×10^5 cps while the maximum counting
rate observed in this wxperiment was on the order of
4×10^3 cps.   Hence, the system was not being paralyzed
by a high counting rate and capable of responding to
successive events.

·The efficiency of a neutron counter is defined as the
fraction of the neutrons which, upon entering the counter,
result in a count.   The probability of the absorption of
a neutron passing a distance d throught the B^{10} is

1-exp(-Ned), assuming a collimated beam of monoenergetic neutrons (Price, 1958). N is the number of B^{10} atoms per cubic centimeter and ϵ is the appropriate cross section. In general, the efficiency depends on the size and shape of the counter and on the direction of incidence of the neutrons as well as the other properties of the counter. In fig. 4, the efficiency is depicted for the counter used in this experiment (96% enriched) for neutrons incident perpendicular to the counter and for those parallel to the counter. The efficiency for various energies has the form

$$\text{Efficiency} = 1 - \exp[-0.624d(0.025/E)^{\frac{1}{2}}]$$

where E is the neutron energy in electron volts.

The measured fast neutron scintillator efficiency is shown in fig. 5 (Haymes, 1965); it follows the shape of the elastic-scattering cross section on energy above the electronically-set threshold of 1 Mev.
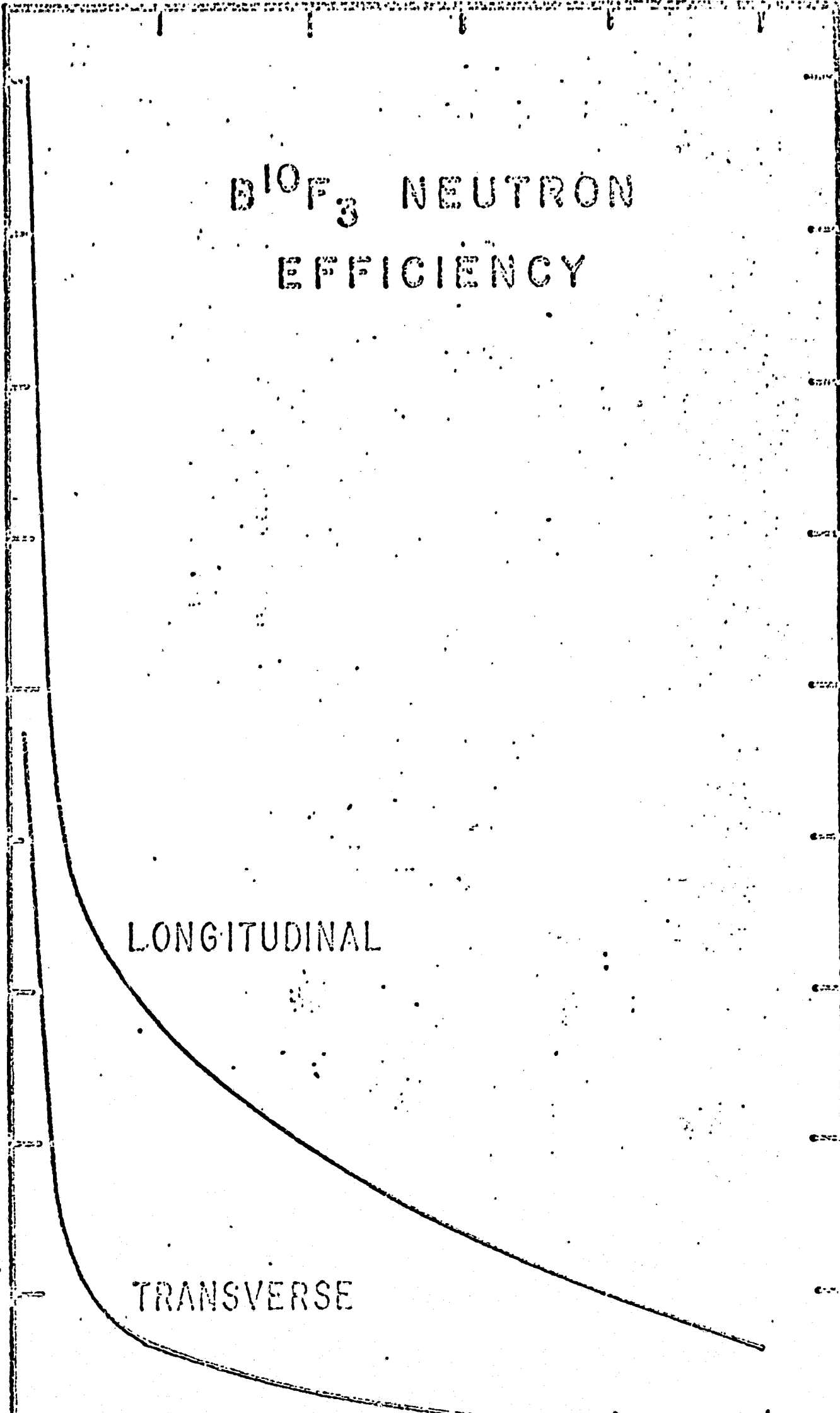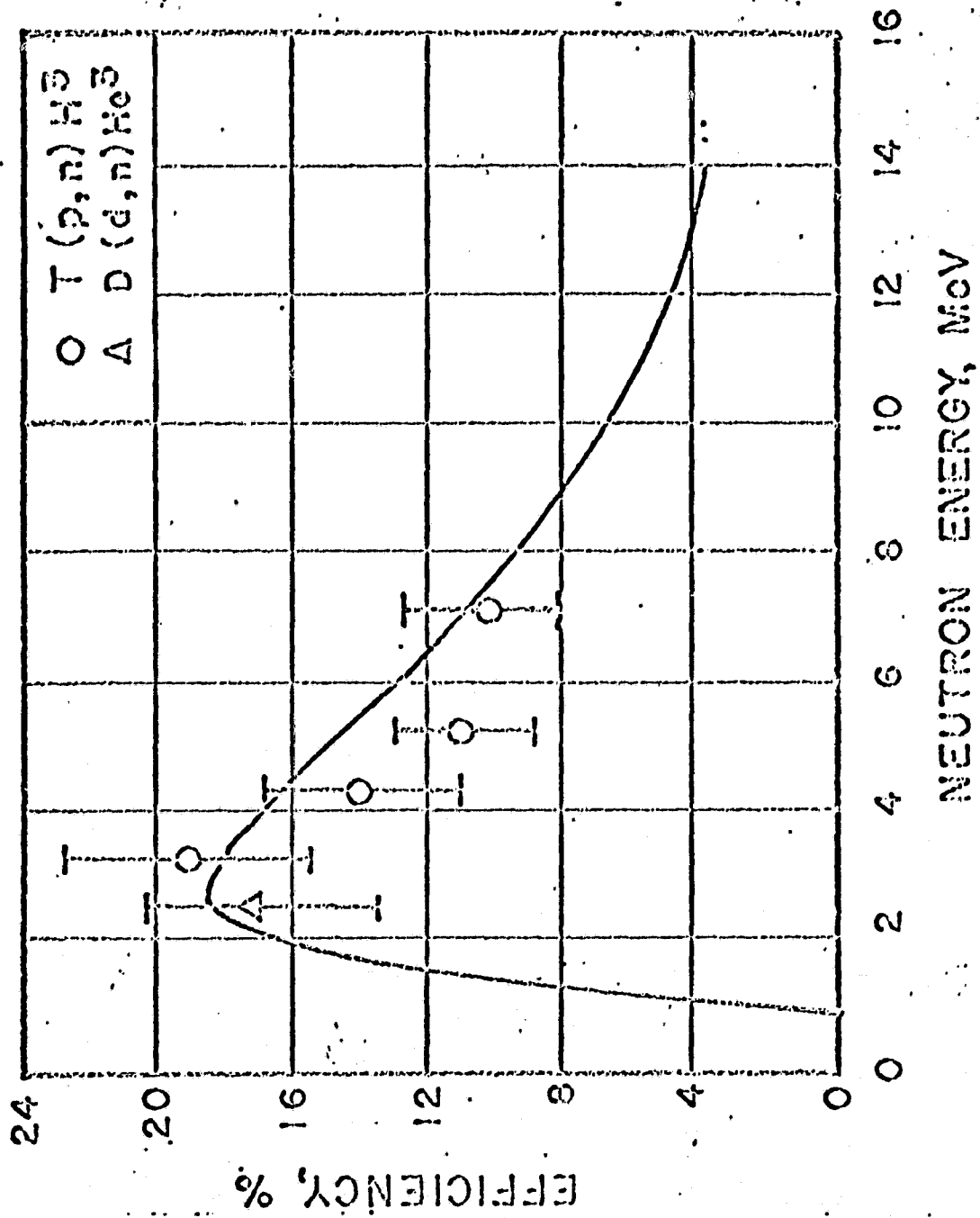
$B^{10}F_3$ NEUTRON EFFICIENCY

Figure 5. Calibration curve of the detector, obtained with monoenergetic neutrons. Calibration with a Pu—Be source yielded 16 ± 5 per cent, an average energy of 4 to 5 Mev.

D.   Experimental Procedure

The objective of this experiment was to measure the slow neutron counting rate, the fast neutron counting rate, both at a given (and measured) water content in the material. As previously stated, the simulator was positioned in the vertical mode when obtaining the counting rates. This was to insure that the counters and the neutron source were entirely covered. Counting rates were obtained and normalized to five minute time segments. Due to the high counting rate, good statistics were obtained.

After the counting periods were made, the simulator was placed into the horizontal mode. Samples were then taken of the material at various positions in the simulator. These samples, ranging between 10-20 grams, were then weighed using an analytical balance. Each of the samples were weighed to the nearest milligram. The weighing was also ± 1 mg. Thus taking large samples reduced the relative errors to a minimum.

The samples were then heated to a temperature of approximately 600 degrees F for several hours until a constant weight was obtained. A dessicator was used to dry and cool the samples before reweighing. The weight loss then was recorded.

The determination of water content involves many factors such as particle size, chemical composition, and type of water binding. The basaltic material used had a chemical composition as depicted in fig. 16. The water contained in this material as indicated is water of

crystallization. The analysis given was based on 105 degrees centigrade. However, in an area where the relative humidity is high, this substance will have absorbed water (Skoog, 1962) which is easily driven off by heating to 105 C. There is also occluded water which occurs in microscopic pockets in the rock material.

At 600 degrees F, all of the absorbed water and water of crystallization will be driven out; some of the occluded water will also be lost. Since carbon dioxide is also driven out of the material, some correction might have to be made in the analysis through weight-loss. However, before the experiment began, the entire basaltic material was heated to 600 F in order to start from a low water content. Therefore, no corrections were required.

The other sample, sand, required no initial heating since it had a low water content ($< 0.1\%$). In fig. 6 the weight loss as a function of temperature is given (Nutting, 1943). In sand, the carbon dioxide driven off at 600 F is negligible compared to that of water.

The background which was present in the slow neutron counting system was primarily due to gamma rays produced in the fast neutron source. Cosmic rays add to the background; roughly one per minute will cross every square cm of horizontal sectional area near sea level (Korff, 1955). Natural contamination from the counter is negligible compared to the other sources. Finally, background due to local radioactive materials and the basaltic and sand materils give a small addition to the background. The background was less than 2% of the B^{10}

WEIGHT LOSS ⟷ TEMPERATURE (NUTTING, 1943)

WEST TEXAS VOLCANIC ASH

SiO₂

10x
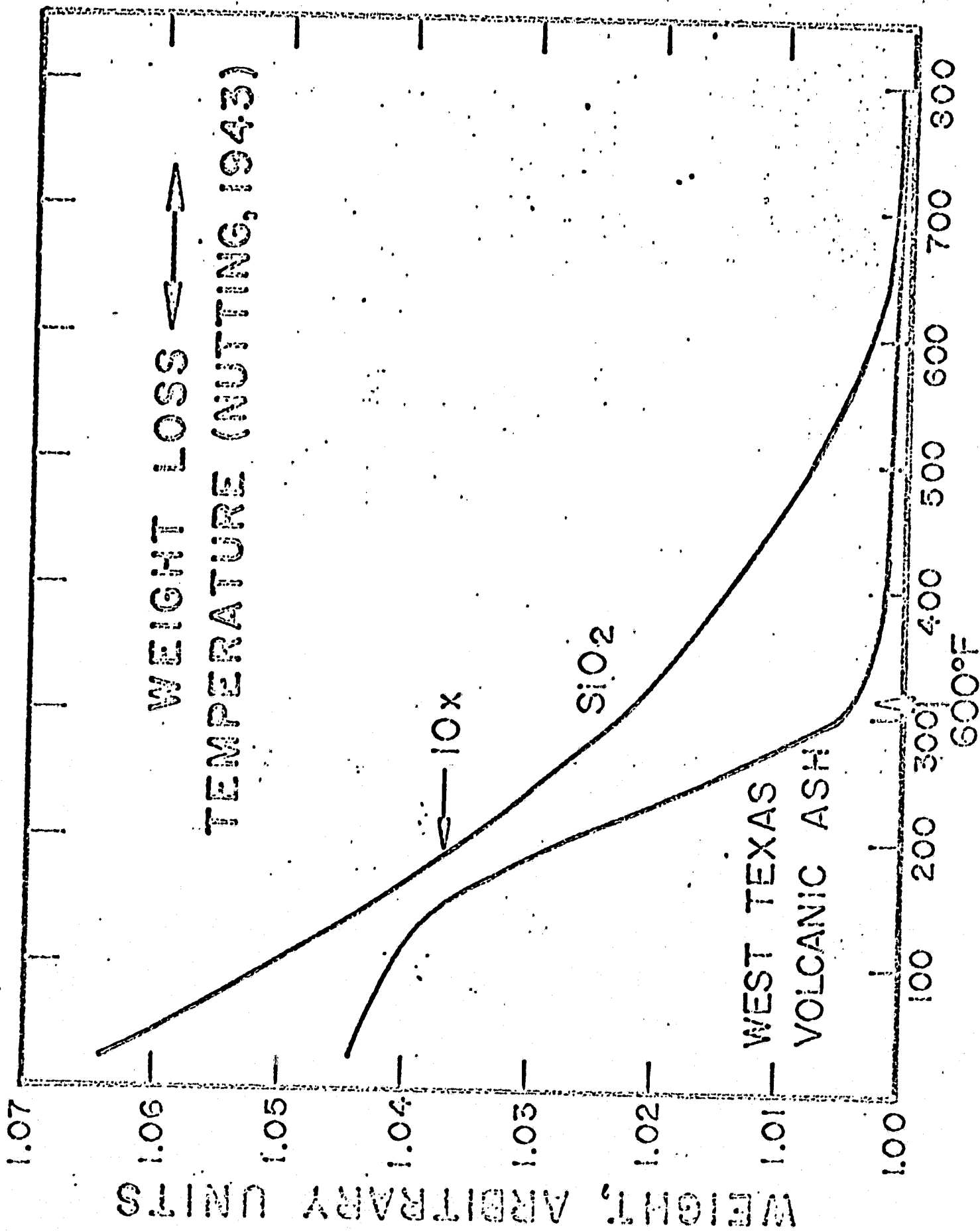
WEIGHT, ARBITRARY UNITS

1.07
1.06
1.05
1.04
1.03
1.02
1.01
1.00

TEMPERATURE °C

100 200 300 400 500 600 700 800

600°F

Fig 6

counting rate. Of this value, more than 90% was due to
the neutron source inside the simulator.

The distribution of neutron energies and fluxes can
be anticipated by use of the diffusion parameters. The
slowing down length, defined as the average shortest
distance that a neutron travels in slowing down from some
energy to another (Isbin, 1964), is comparable to the
source-detector distance. A value of approximately 9
inches in basalt indicates that in the energy range of
the 4 Mev average [Beckurts, 1964] source energy to ther-
mal energies, the neutrons are thermalized. However, the
very high energy neutrons are not thermalized in this
range, but are in the epithermal range. For closer source-
detector distances, the counting rate will increase because
the slow neutron density increases approximately as $1/r$
(Title, 1964).

As water is added to the material, the neutrons
which are slowed down to the epithermal energies begin
to be further slowed down, hence they are counted. This
also will cause some of the faster neutrons to be slowed
down so that they will not be counted by the fast counter.

In fig. 7 the counting rates for the source-detector
distance are shown. Outside the simulator, the flux is
approximately 1/10 that of the 1.5" distance flux and
represents the leakage from the simulator. The fluxes
computed by diffusion theory and the resulting counting
rates for thermal neutrons are comparable.

In fig. 8 the counting rate is plotted versus the
depth below the top level of the medium. This indicates
that the center of maximum slow neutron activity does

NEUTRON FLUX
n-p + Bi0
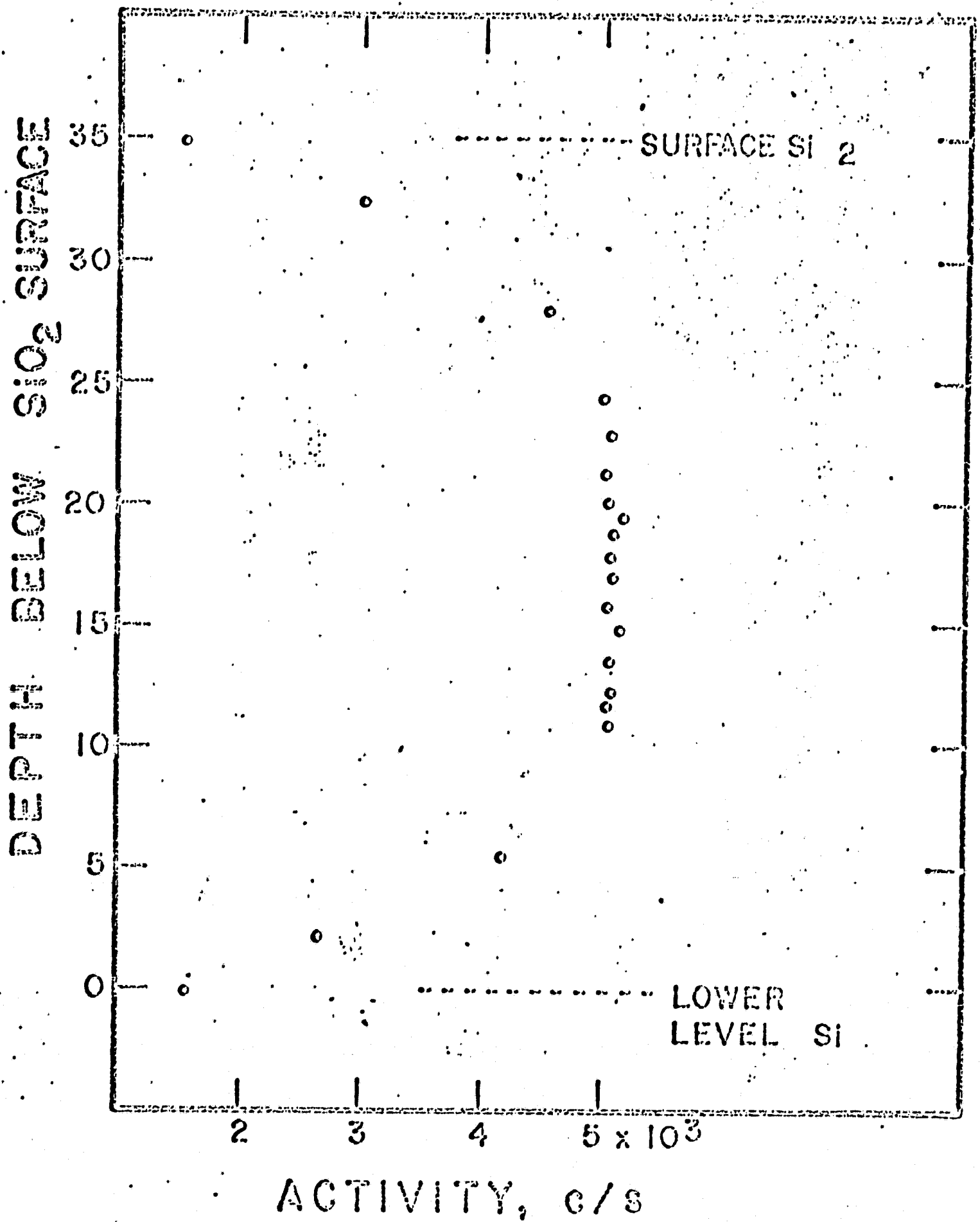
SN(Bi0)

FN(n-P)

cpm

10⁵
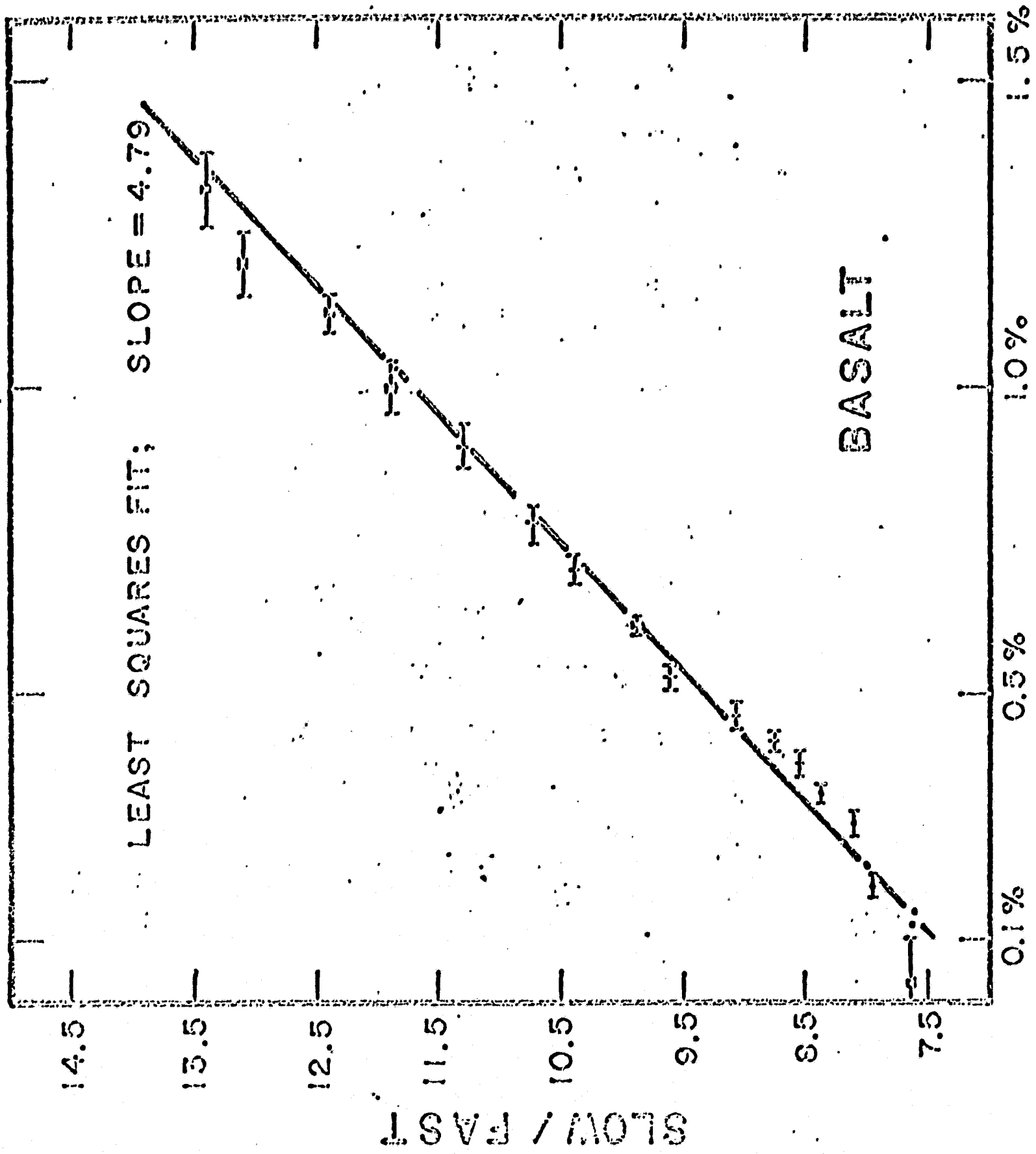
10⁴

10³

9.5"   18"
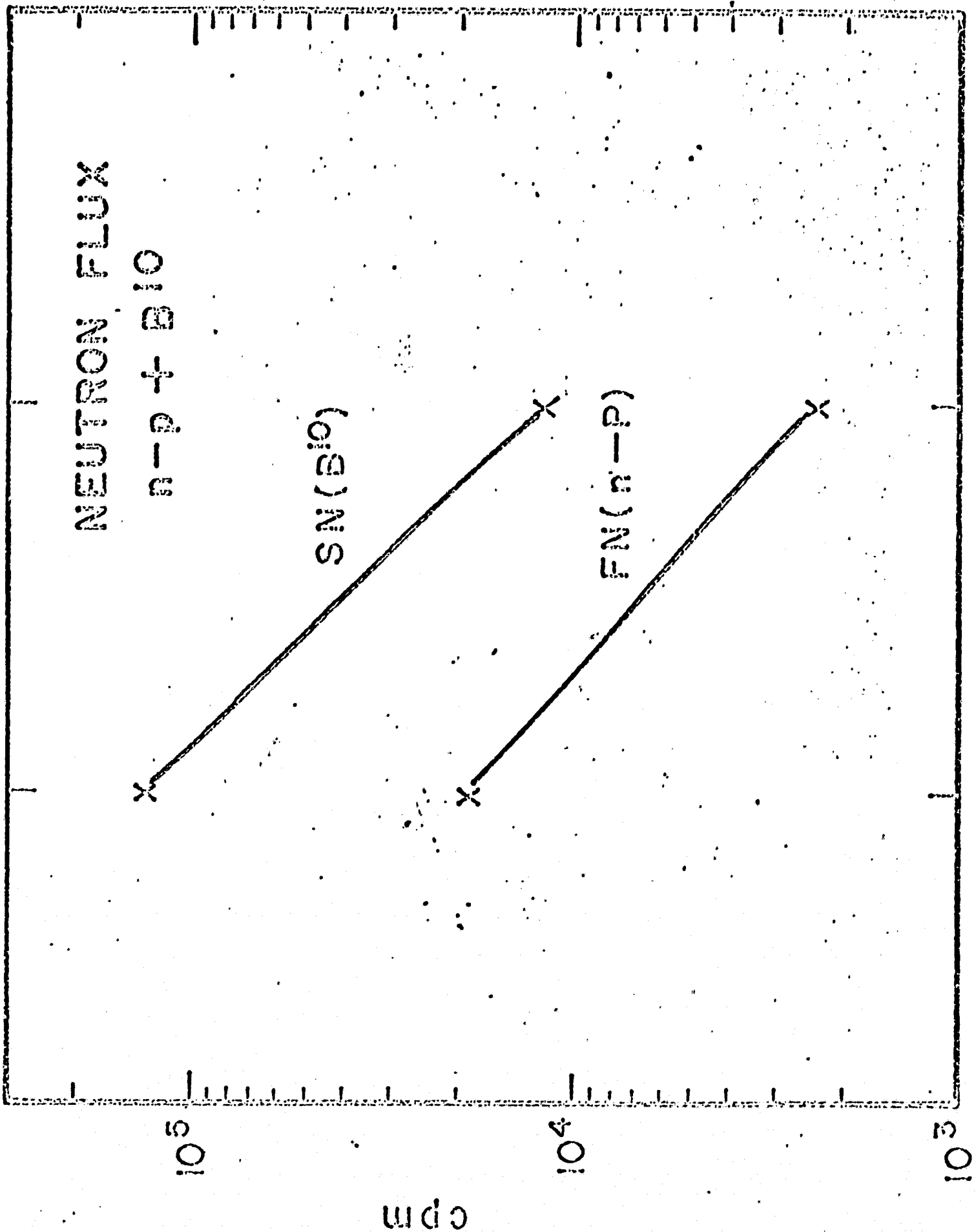
Fig 8

not vary appreciably over the ranges indicated. Hence, the levels of both the sand and the basalt are not required to exactly coincide, physically.

This is also an indication of the thermalization that is present; the small variations observed are not statistically significant. If the neutrons were not completely thermalized, then a small change in the source-detector distance would give an appreciable change in counting rates.

E.   <u>Results</u>

In figs. 9 and 10, the ratio of slow to fast neutron counting rates corresponding to the equivalent water content ate depicted. A least squares fit of a linear curve to the data gives a slope of 4.79/%H_2O for basalt and 2.22/%H_2O for sand. The standard deviation of the observed counting rates is very small due to high counting rates and long exposure times. The standard deviation of the water content values varies due to irregularities in the mixing process, such deviations for the sand are much lower than those measured for basalt. This is because the sand is much easier to mix with the water. The composite counting rates are plotted in figs. 11 and 12.

The difference in the slopes of the curves in figs. 9 and 10 can be attributed to two factors. One is that the slowing down length of the neutrons in the sand is longer than that of the basalt, so that there are fewer thermal neutrons to count. This is seen in the counting rates in fig. 12. There is a higher flux of epithermal neutrons that are then affected considerably by the addition of water. A more noticeable increase in the counting rate is consequently produced. The other factor is that the basalt has a higher cross section for absorption than the sand (see fig. 16 for chemical analysis). This will tend to cause more thermal neutrons to be extracted from the medium, hence, the counting rates are also affected.
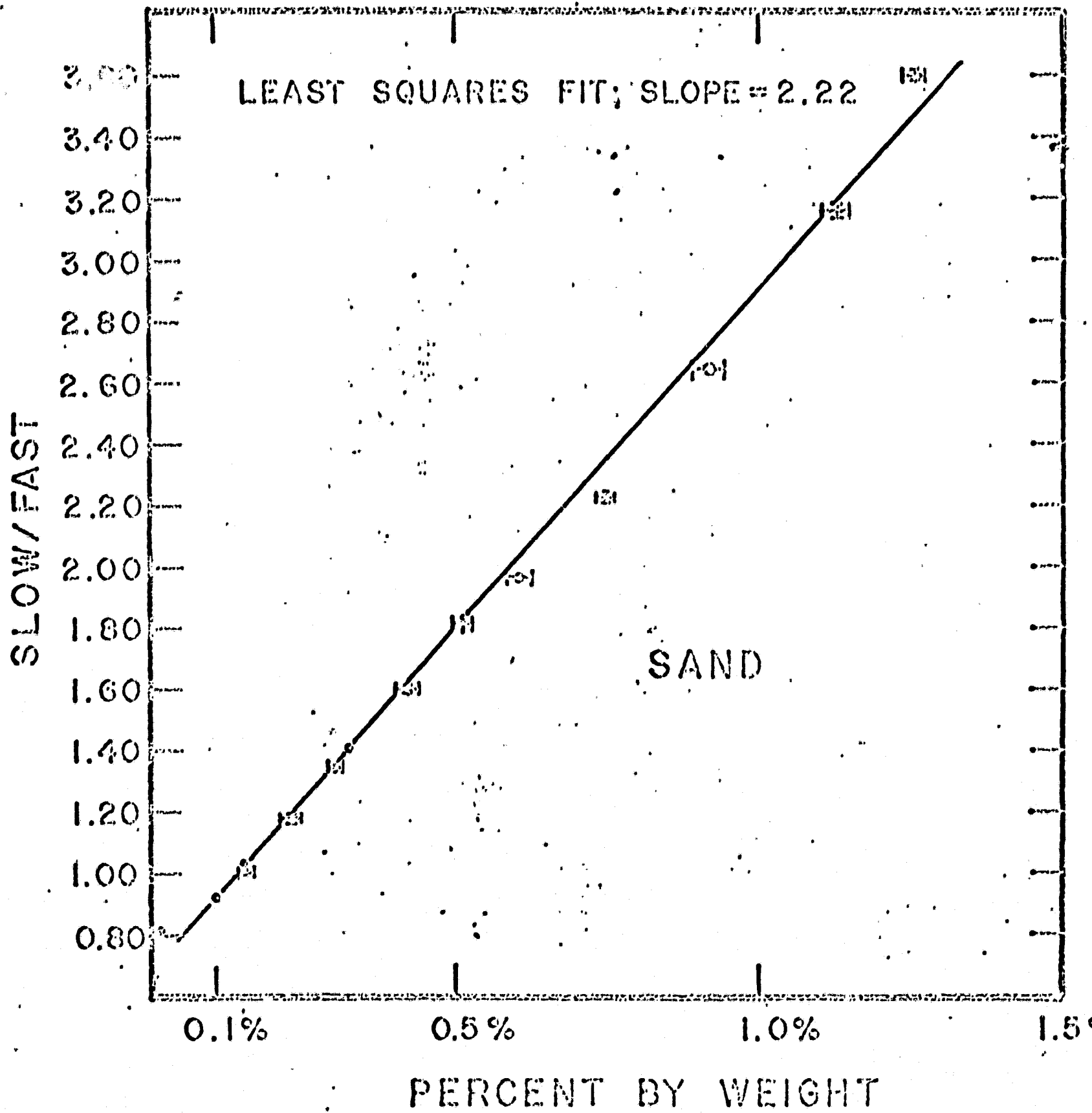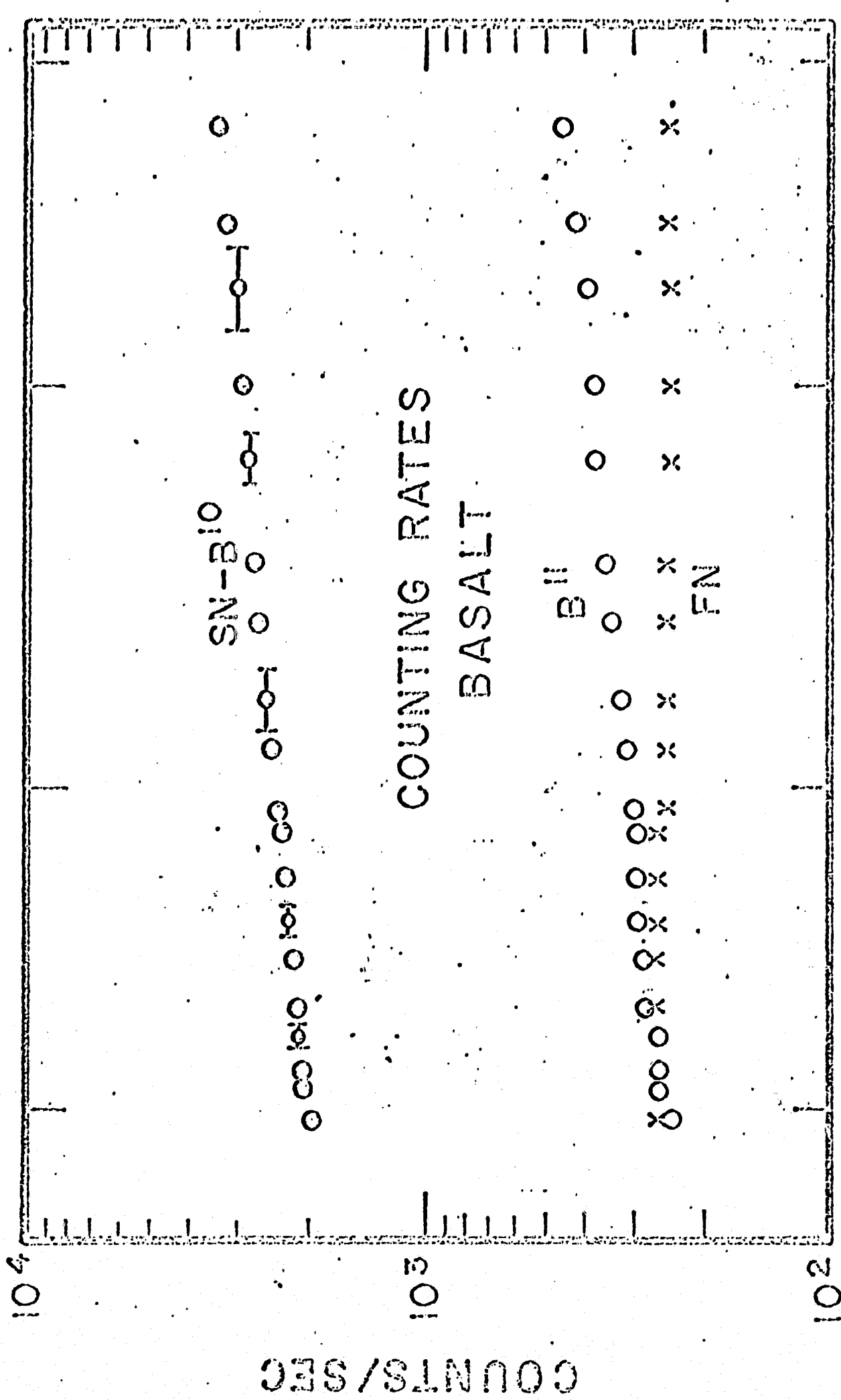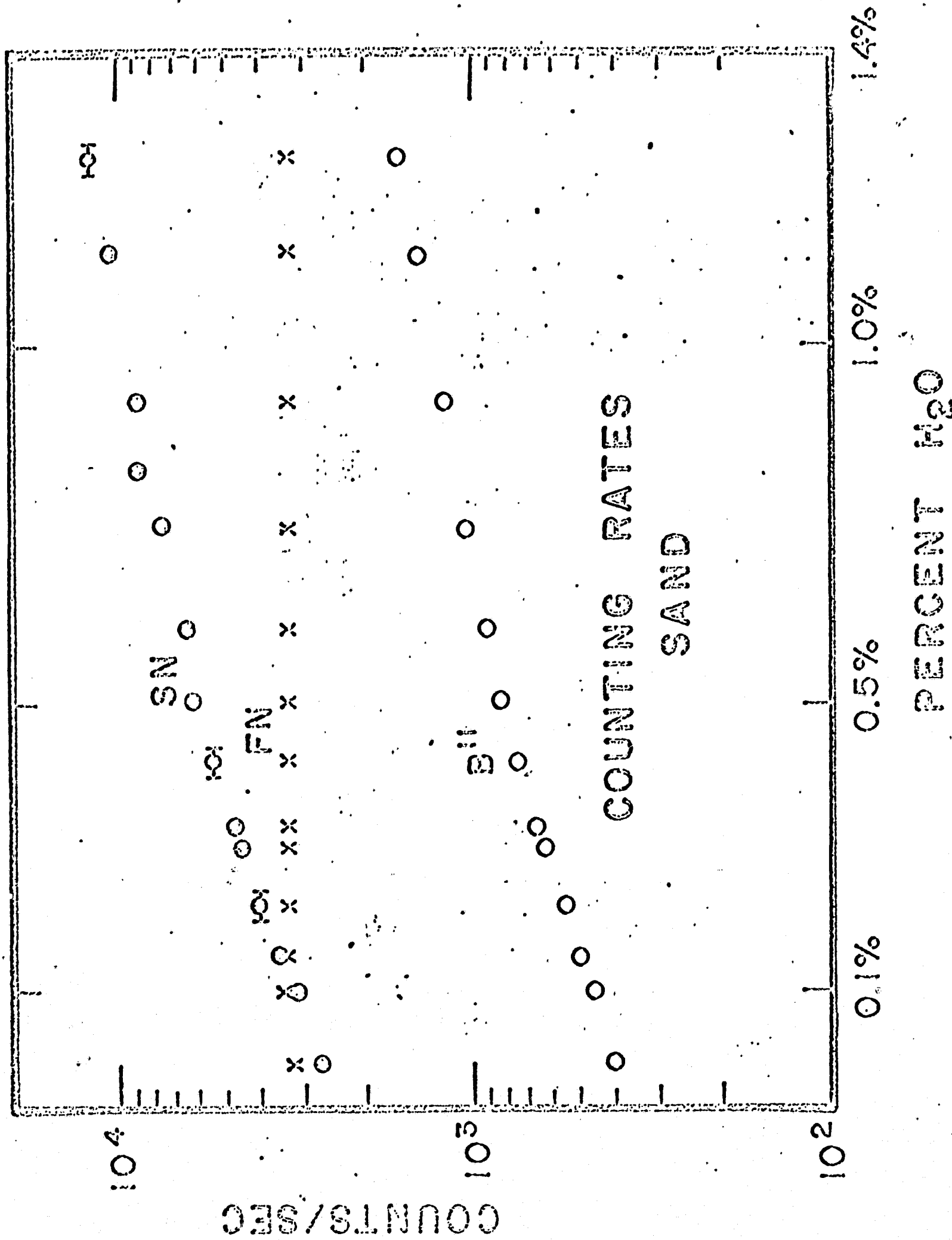
LEAST SQUARES FIT; SLOPE = 4.79

BASALT

Fig 10

COUNTING RATES
BASALT

SN-B10

B11

FN

PERCENT H2O

Fig 11

COUNTS/SEC

COUNTING RATES

SAND

PERCENT H2O

III. DISCUSSION

A. The Lunar Neutron Flux

Lingenfelter, Canfield and Hess (LCH) have calculated the cosmic ray induced neutron leakage spectrum for various assumed lunar compositions. The equilibrium spectrum is shown in fig. 13. According to this analysis, hydrogen may be detected if the ratio of H/Si = 0.05. This corresponds to chondrites of .3% water by weight. It was assumed by LCH that the surface of the moon was similar to chondritic material which has a composition similar to basic rocks of the Earth.

The ratio of H/Si = 0.05, which also is 0.25 gm/cm^2 in the upper 100 gm/cm^2 of the lunar crust, is dependent on the cross section of thermal absorbers and uncertain in LCH's calculation of ± 50%. The Surveyor missions have determined the chemical composition and hence the thermal-neutron cross section to ± 7%. With this value, the ratio of H/Si will be known to about ± 10%. (In general, the value of the H/Si ratio can be determined to nearly the same accuracy as the uncertainty in the total capture cross section for H/Si 0.1, LCH, 1961).

The following relation between mineral type and the fraction of neutrons which leak into space holds:

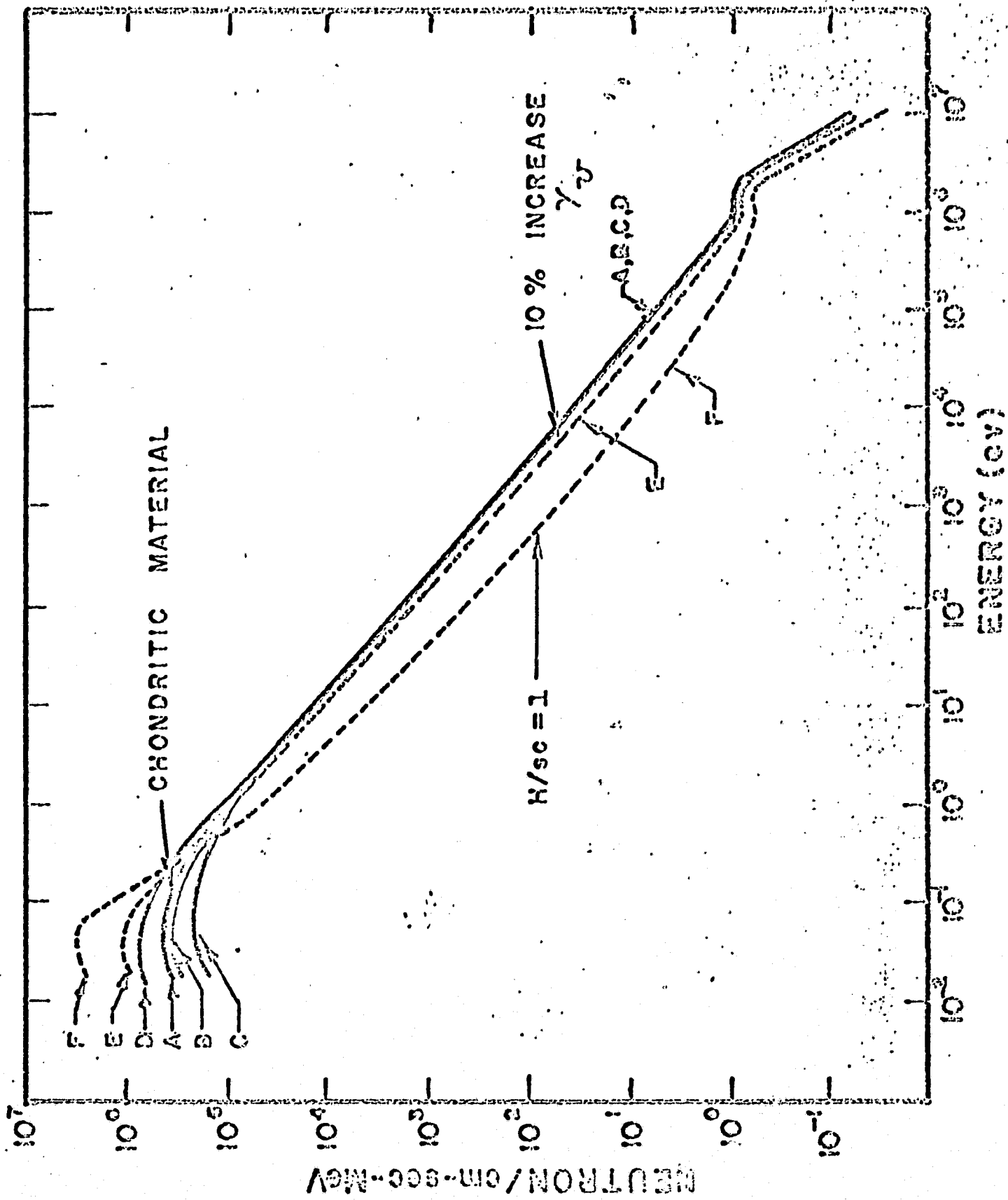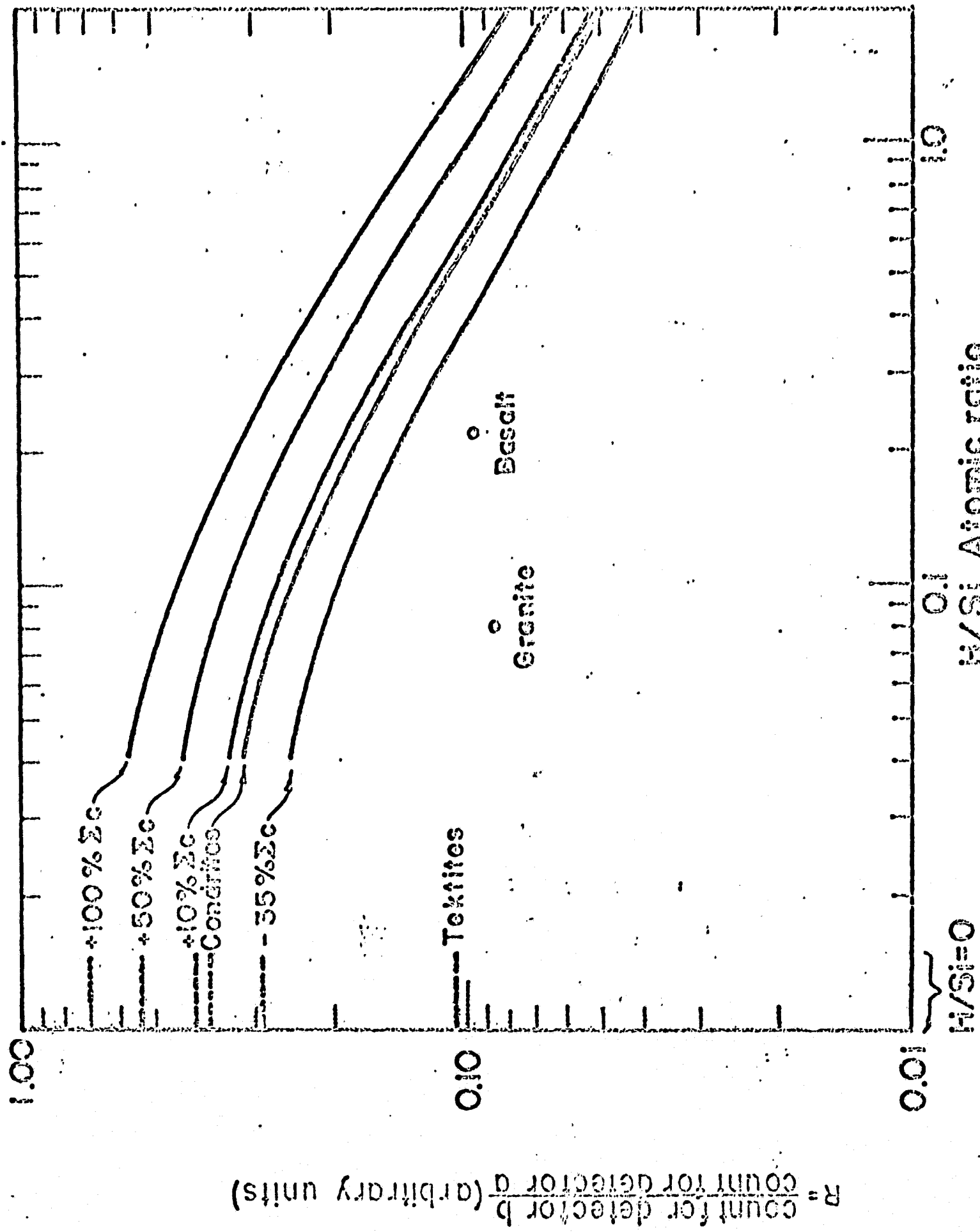| Mineral Type	Neutron Leakage
Chondrites	35.9%
Basalt	29.7
Granite	32.3
Tektites	40.0

Fig 13

Fig. 16

For chondritic material, the leakage decreases to
30.3% with the addition of 0.1 hydrogen atom per silicon,
and 17.3% with 1.0 hydrogen per silicon (LCH, 1961). The
leakage is quite insensitive to changes in the capture
cross section; a 35% decrease in capture cross section
yielding only a 0.6% increase in the leakage, and a 50%
increase yielding only a 0.7% decrease.

In fig. 14 the calculated neutron counting rate
ratios for a $B^{10}F_3$ proportional counter and the same
detector with a flat response at higher energies by
using a moderator are shown. Two detectors are needed
in the lunar experiment due to the uncertainty in the
absolute source strength and the thermal cross section
for absorption (LCH, 1961)

B.   The Surveyor Experiments

   The results of the alpha-scattering analyses of the
top layers of the moon's surface (Turkevich, 1967) provides
us with the chemical composition at the landing sites of
Surveyors V, VI, and VII (fig. 15).   The hydrogen concen-
tration cannot be estimated from an alpha-scattering
experiment.   In fig. 17, the measurements of the lunar
composition are shown, and in comparison, in fig. 18 the
chemical analysis of the materials used in this experiment
are shown.

   The Surveyor V and VI landings were in the maria
regions while Surveyor VII was performed in a highlands
site.   The results indicate that the composition is clearly
different from that of chondrites and resembles that of
terrestrial basalts.   The VII analysis shows a marked
difference from the other two analyses in that the iron
content is distinctly less (the "Fe" peak in the Surveyor
analyses also include neighboring elements).

   LCH's calculations were primarily based on the
chondritic theory of the moon.   Chondrites, which are
stony meteorites, were linked with a parent body, possibly
the moon.   Hence, this theory needs to be revised and LCH's
calculations based on the basaltic composition.
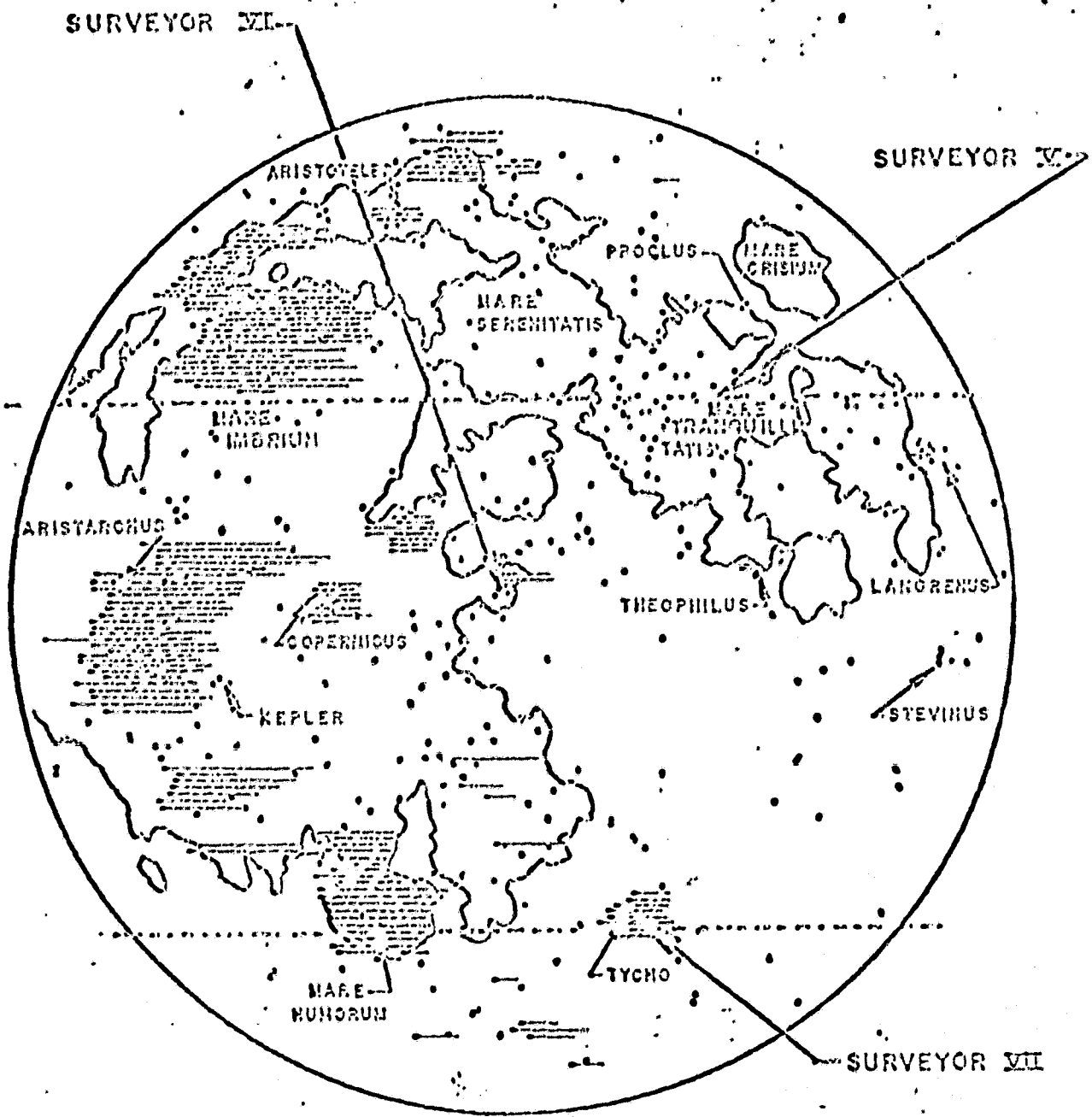
SURVEYOR LANDING SITES

Fig 15

ANALYSIS

	Wt. %, 105°C basis	
	Basaltic Rock	Sand
SiO_2	45.09	95.40
Al_2O_3	5.87	3.22
CaO	13.94	0.06
MgO	13.64	0.03
FeO	6.87	-
Fe_2O_3	3.23	0.11
TiO_2	3.60	0.09
K_2O	1.13	0.83
Na_2O	2.56	0.12
BaO	0.09	0.03
SrO	0.13	0.002
NiO	0.05	-
CuO	0.008	0.005
ZnO	0.016	0.004
Nb_2O_5	0.01	-
Rb_2O	0.002	-
ZrO	0.04	0.03
Y_2O_5	0.004	-
H_2O+	2.52	-
CO_2	0.75	-
	99.700	99.931

Fig 15

ELEMENT	SURVEYOR V	SURVEYOR VI	SURVEYOR VII
CARBON	< 3 %	< 2 %	< 2 %
OXYGEN	58 ± 5	57 ± 5	58 ± 5
SODIUM	< 2	< 2	
MAGNESIUM	3 ± 3	3 ± 3	4 ± 3
ALUMINUM	6.5 ± 2	6.5 ± 2	8 ± 3
SILICON	18.5 ± 3	22 ± 4	18.5 ± 3
"CALCIUM"		6 ± 2	6 ± 2
"IRON"	13 ± 3	5 ± 2	2 ± 1

Measurements of Lunar Composition at Landing Sites of Surveyors V, VI, and VII

FIG 1.7

C.   The Lunar Neutron Experiment

American Science and Engineering has prepared a
report (ASE-1919) for the National Aeronautics and Space
Administration for a proposed lunar surface exploration
experiment. Part of this experiment will concern the
measurement of the lunar neutron flux. This will be an
orbital experiment in a near-moon orbit; the orbital
velocity would be about 1.7 km/sec. In a thirty second
time interval, an omnidirectional detector will scan a
path on the lunar surface of about 50 km in length (the
altitude is about 20 nautical miles).

For a basaltic lunar composition, a change in the
water concentration from 0.2% - 0.3% would result in about
a 4% change in the slow counting rate (assuming the fast
component is constant). For the satellite experiment to
see this change, one must look at the expected counting
rates. Using the LCH value of a neutron strength approxi-
mately five times that of the Earth's atmosphere, and
using (Haymes and Korff, 1960) the slow neutron density
near the top of the mid-latitude atmosphere to be
approximately 1×10^{-8} neutrons/cm^3, a counting rate of
900 c/min is expected. A background of charged particles
(using the values near the Earth's poles) is about 1000
c/min. These counting rates assume that the detectors
employed are similar to those in this experiment. The
values for the B^{10} counter would be about 1900 c/min and
1100 c/min for the B^{11} counter.

IV. CONCLUSIONS

The principal results of the lunar neutron albedo feasibility
study are shown in figs. 9 and 10. These data show that statistically-
significant deviations in the ratio of the slow to fast neutrons
result when the hydrogen concentration in the sample is only slightly
changed.

One consequence of the Surveyor lunar alpha-scattering experiments
is that basalt provides a good mockup of the lunar surface material.
A change of 0.2 - 0.3% in water content (which represents the
chondritic water content by weight) would produce a change in
the slow counting rate of about 4%, using a basalt from West Texas
(the fast component in this experiment was seen to be constant to
a first approximation).

In a thirty second integration time, an area of ~50 km on
the moon would be swept out. A proposed lunar orbiting experiment
would see a neutron counting rate of approximately 1900 c/min for
the slow B^{10} counter. A probability of 0.8 exists that a 4% change
in the ratio would be detected, even in a single pass over an area
this size.

REFERENCES

Beckurts, K. H., Nuetron Physics, Springer, New York (1964)

Feld, B. T., "The Nuetron": Part VII of Experimental Physics, V. 2, John Wiley and Sons, Inc., New York (1953)

Fichtel, C. E., Solar Proton Manual, NASA Tech. Rept. TR-R169 (1963)

Skoog, D. A., West, D. M., Analytical Cehmistry, pp. 712-718, Holt, Rinehart & Winston, New York (1963)

Glasstone, S., and Edlund, M. C., Elements of Nuclear Reactor Theory, pp. 56-59, Van Nostrand, Inc., Princeton, N. J. (1952)

Gorenstein, P., "Lunar Surface Exploration by Satellite", ASE-1919 Report (1968)

Green, J., North American Aviation Corporation Unpublished Internal Report (1964)

Haymes, R. C., and Korff, S. A., "Slow-Neutron Intensity At High Balloon Altitudes", Phys. Rev., 120, 1460-1462 (1960)

Haymes, R. C., "Fast Neutrons In The Earth's Atmosphere", 1. Variation With Depth, J. Geophys. Res., 69, 841-852 (1964a)

Isbin, Herbert S., Nuclear Reactor Theory, pp. 54-61, Reinhold Publishing, New York (1963)

Korff, S. A., Electron and Nuclear Counters, pp. 23-25, Van Nostrand Company, New York (1946)

Lingenfelter, R. E., Canfield, E. H., Hess, W. N., "Lunar
    Neutron Flux", J. Geophys. Res., 66, 2665 (1961)

Nutting, P. G., U. S. Geological Survey, Professor Paper
    197-E (1943)

Price, William J., Nuclear Radiation Detection, pp. 28-39,
    McGraw-Hill, New York (1958)

Rusk, Rogers D., Atomic and Nuclear Physics, pp. 376-380,
    Appleton-Century-Crafts, New York (1964)

Soodak, Harry, Elementary Pile Theory, J. Wiley, New York
    (1950)

Title, C. W., "Neutron Transmission and Diffusion", Nuclear
    Chicago Bulletin No. 10, Nuclear-Chicago Corporation
    (1964)

Turkevitch, A., Patterson, J. H., "Surveyor V", Science,
    631, Nov. 3 (1967)

Watson, K., Murray, B., Brown, H., "Presence of Ice on
    the Moon", J. Geophys. Res., 66, 1598 (1961)